Journal of Electronic Research and Application, 2026, Volume 10, Issue 4
http://ojs.bbwpublisher.com/index.php/JERA
Online ISSN: 2208-3510
Print ISSN: 2208-3502

Design of UWB-AOA Circularly Polarized Antenna for Automotive Digital Key Systems

Binghao Zeng[1]*, Jinhai Wu[1], Xiong Huang[1], Yunfeng Zhou[1,2]

[1]Shenzhen Sunnyway Technology Co., Ltd., Shenzhen 518000, Guangdong, China
[2]Shanghai Sunnyway Communication Technology Co., Ltd., Shanghai 201702, China

Author to whom correspondence should be addressed.

Abstract: This paper designs an ultra-wideband (UWB) circularly polarized antenna based on Angle of Arrival (AOA) positioning technology. The antenna element adopts a rectangular dual-feed microstrip patch structure, and realizes right-hand circular polarization (RHCP) radiation through a 90° feeding network, which effectively suppresses vehicle multipath interference and polarization mismatch problems; a compact L-shaped three-antenna array is built based on the elements, and the array layout and feeding network are optimized to ensure phase and amplitude consistency. The simulation analysis results show that the operating frequency band of the antenna element can completely cover 6.24~8.24 GHz, with a return loss of ≤ -10 dB and an axial ratio of ≤ 3.0 dB within this band; the isolation between ports is ≤ -21dB, the gain is stable at 3.55–5.05 dBi, and the AOA positioning error is ≤ 1.4° (positioning distance 0.5–5 m). The overall size is controlled at 42mm × 30mm × 2mm, which fully meets the application requirements of automotive digital keys for miniaturization, high precision, and anti-interference. It can be directly integrated into digital key terminals, improving the reliability of contactless unlocking and the security of anti-theft authentication.

Keywords: UWB-AOA; Automotive digital key; Circularly polarized antenna; Dual-feed microstrip patch; L-shaped array

Online publication: May 21, 2026

1. Introduction

With the in-depth iteration of automotive intelligent and connected technologies, automotive digital keys, as upgraded alternatives to traditional mechanical keys and remote-control keys, have become core terminal components of modern automotive intelligent by virtue of their core advantages such as contactless unlocking, remote start, personalized adaptation, and anti-theft authentication, and are widely used in various passenger vehicles.

Currently, the positioning and communication technologies for automotive digital keys are mainly divided into three categories: Radio Frequency Identification (RFID), Bluetooth Low Energy (BLE), and

UWB. Among them, RFID technology has low positioning accuracy, is easy to crack, and has insufficient anti-theft performance. Bluetooth technology has weak anti-multipath interference capability, and its positioning accuracy drops significantly in complex in-vehicle environments, making it difficult to meet the requirements for close-range precise unlocking and anti-theft authentication [1].

UWB technology has become the preferred technical solution due to its unique advantages, including an ultra-wide operating frequency band of 3.1–10.6GHz, nanosecond-level time resolution, centimeter-level positioning accuracy, strong anti-electromagnetic interference capability, and difficulty in being cracked. The automotive digital key antenna mainly operates in the frequency band from 6.24 GHz to 8.24 GHz, specifically with Channel 5 (6.4896 GHz) and Channel 9 (7.9872 GHz) as the core operating frequency points. These two frequency bands are clearly specified by the Car Connectivity Consortium specifications to ensure the high-precision positioning and security of digital keys [2,3].

AOA positioning technology, as the core implementation method of UWB positioning, calculates the target's angle of arrival through the phase difference of signals received by the array antenna, enabling accurate identification of the orientation and distance of the digital key relative to the vehicle. Currently, most UWB antennas for automotive digital keys adopt a single-feed circular polarization structure. Although they have the advantage of simple structure, they have shortcomings such as narrow axial ratio bandwidth, insufficient polarization purity, and limited ability to resist multipath interference [4–7].

This paper designs a UWB-AOA circularly polarized array antenna suitable for automotive digital key scenarios, using a rectangular dual-feed UWB circularly polarized array element and a 90° feeding network. The antenna is composed of a compact L-shaped three-antenna array, and the layout is optimized to ensure phase and amplitude consistency, achieving a coordinated improvement of antenna performance and the requirements of digital key scenarios [8,9].

2. Antenna theory and design

2.1. Theory of circularly polarized antennas

The formation of a circularly polarized wave requires two orthogonal linearly polarized electric fields to have equal amplitudes and a phase difference of 90°. This characteristic can effectively solve the problems of polarization rotation and polarization mismatch caused by signal reflection from vehicle body metals and the ground in vehicle-mounted scenarios, isolate reflected multipath signals with opposite rotation directions, and improve the ability to resist multipath interference. This paper adopts a rectangular dual-feed microstrip patch structure to achieve circular polarization. A 90° feeding network is used to provide excitation signals with a phase difference of 90° for the two orthogonal feed points, enabling the radiating patch to generate two orthogonal linearly polarized electric fields, which then synthesize RHCP radiation [10]. For a rectangular microstrip patch element, its resonant frequency can be expressed by **Equation (1)**:

$$f = \frac{c}{2L_{eff}\sqrt{\varepsilon_{reff}}} \tag{1}$$

In the formula, c is the speed of light in vacuum (3×10^8 m/s), L_{eff} is the effective length of the radiating patch, and the handwritten $å_{reff}$ is the effective dielectric constant of the substrate [11,12]

As shown in **Figure 1**, in the dual-fed circularly polarized microstrip antenna, feeding is performed at feeding terminals A and B, which can excite two linearly polarized waves with equal amplitude and a phase

difference of 90°, thereby achieving circular polarization [13–15].

The relevant calculation formulas are as follows:

$$\varepsilon_{reff}=\frac{\varepsilon_r+1}{2}+\frac{\varepsilon_r-1}{2}\left(1+\frac{12h}{W}\right)^{-\frac{1}{2}} \tag{2}$$

$$W=\frac{c}{2f}\left(\frac{\varepsilon_r+1}{2}\right)^{\frac{1}{2}} \tag{3}$$

$$L=\frac{c}{2f\sqrt{\varepsilon_{reff}}}-2\Delta L \tag{4}$$

$$\Delta L=0.412h\frac{\left(\varepsilon_{reff}+0.3\right)\left(\frac{W}{h}+0.264\right)}{\left(\varepsilon_{reff}-0.258\right)\left(\frac{W}{h}+0.8\right)} \tag{5}$$

Here, h is the thickness of the dielectric board, W and L are the width and length of the radiating metal patch, respectively, and $\triangle L$ is the length of the equivalent radiating slot.

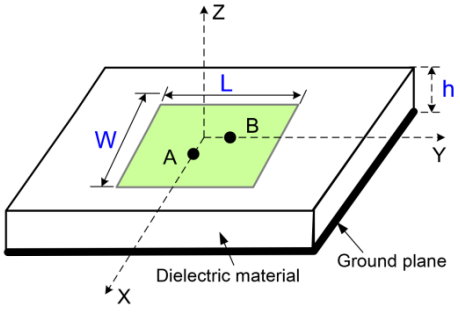

Figure 1. Microstrip antenna structure.

2.2. 2D AOA calculation for L-shaped arrays

An L-shaped orthogonal three-antenna array realizes the two-dimensional Angle of Arrival (AOA) estimation of UWB signals. The array takes Ant. 1 as the coordinate origin, Ant. 2 is arranged along the x-axis, and Ant. 3 is arranged along the y-axis, with the spacing between array elements all being d. When a far-field plane wave is incident at an azimuth angle θ, due to the different positions of each antenna, there is a path difference when the signal reaches each antenna unit, which is then converted into a measurable phase difference. Finally, the incident angle of the signal is calculated through the arctangent function. The principle of the L-shaped three-antenna UWB two-dimensional AOA is shown in **Figure 2**. The relevant calculation formulas for the process are as follows:

The path differences is:

$$\Delta r_{12}=d\cos\theta \tag{6}$$

$$\Delta r_{13}=d\sin\theta \tag{7}$$

Here, r = the path (distance) of wave propagation, which is the path difference between Ant. 1 and Ant. 2; the uppercase Delta r with subscript 13 is the path difference between Ant. 1 and Ant. 3; d is the distance between adjacent antenna elements; theta is the signal incident azimuth angle.

The phase difference has a linear relationship with the path difference, and the phase difference is equal to the product of the path difference and the wave number:

$$\Delta\phi=\frac{2\pi}{\lambda}\Delta r \tag{8}$$

$$\Delta\phi_{12}=\frac{2\pi}{\lambda}d\cos\theta=\frac{2\pi f}{c}d\cos\theta \tag{9}$$

$$\Delta\phi_{13}=\frac{2\pi}{\lambda}d\sin\theta=\frac{2\pi f}{c}d\sin\theta \tag{10}$$

$$\tan\theta=\frac{\Delta\phi_{12}}{\Delta\phi_{13}} \tag{11}$$

To achieve full-angle calculation from 0° to 360° and distinguish quadrants, the four-quadrant arctangent function atan2 is used in engineering:

$$\theta=atan2(\Delta\phi_{13},\Delta\phi_{12}) \tag{12}$$

Using the above formula, the two-dimensional angle of arrival of the signal can be directly solved from the phase difference of the two paths, completing the L-shaped three-antenna UWB-AOA direction finding.

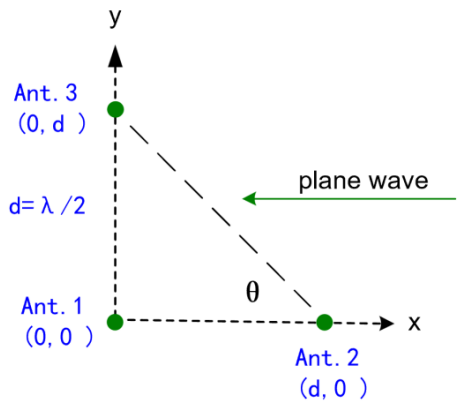

Figure 2. Schematic of far-field plane wave incident on L-shaped array with azimuth angle θ.

2.3. Antenna design and structure

As shown in Figure 3, the specific layout of the three array elements is as follows: The central array element (Ant.1) is located at the corner of the L-shape, serving as the reference unit for AOA positioning and fitting the corner position of the digital key housing; Ant.2 and Ant.3 are respectively located at the ends of two vertical array arms. The length of each array arm is 30mm, fitting the two vertical edges of the digital key housing. The angle between the connecting lines of adjacent array elements is strictly controlled to 90°, with a deviation of ≤ 0.5°, ensuring array symmetry and radiation uniformity to achieve omnidirectional AOA angle estimation.

The distances (d) between Ant.1 and Ant.2, and between Ant.1 and Ant.3 are both 18.5mm, which corresponds to 0.492 times the free-space wavelength λ_0 of the center frequency (7.9872GHz). This distance can effectively balance the mutual coupling between ports, AOA positioning accuracy, array size

compactness, and the installation space requirements of the digital key; the distance between Ant.2 and Ant.3 is approximately 26.16mm, forming a symmetrical L-shaped structure to ensure the uniformity of omnidirectional radiation and the consistency of angle estimation.

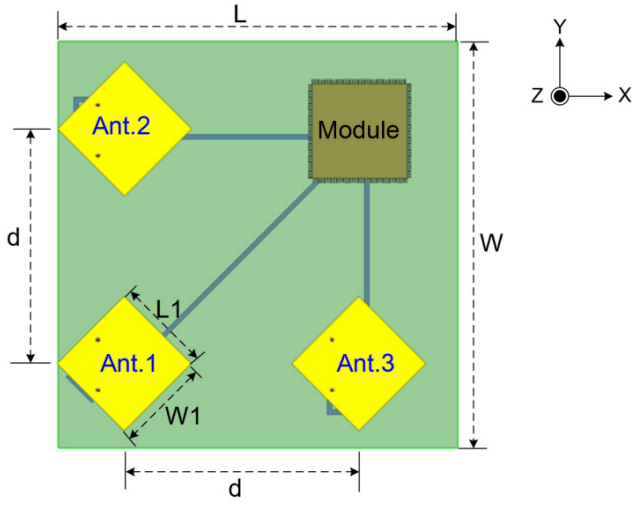

Figure 3. L-shaped three-antenna UWB-AOA construction model.

3. Simulation analysis results

Comprehensive performance simulation tests were conducted on the designed UWB-AOA circularly polarized array antenna. The operating frequency band of the L-shaped three-antenna array element can cover a wide range from 5.80 to 9.0 GHz, which fully includes the frequency band of 6.24 GHz to 8.24 GHz where the car digital key antenna mainly operates. The Return loss in the entire frequency band is ≤ -10 dB, meeting the design requirements, as shown in **Figure 4**. At the core frequency point of 7.9872 GHz, the isolation between ports is ≤ -21dB, which effectively reduces the mutual coupling interference between array elements, as shown in **Figure 5**. The axial ratio within the core frequency band is ≤ 3.0 dB, with excellent polarization purity, which can effectively suppress the problem of vehicle polarization mismatch, as shown in **Figure 6**.

The radiation pattern covers an azimuth angle range of 0° to 360° and an elevation angle range of -35° to 30°, with good radiation performance, as shown in **Figure 7**. In the frequency band of 6.24 GHz to 8.24 GHz, the average radiation efficiency is ≥ 50%, and at the core frequency point of 7.9872 GHz, the average radiation efficiency is ≥ 69.5%, as shown in **Figure 8**. The phase deviation of each channel of the array is accurately controlled within 4°, ensuring the consistency of signal amplitude and phase, and providing a reliable basis for the phase difference calculation of AOA positioning; the gain is stable at 3.55–5.05 dBi, with a fluctuation amplitude of ≤ 1.5 dB, as shown in **Figure 9** [16]. Within the common positioning distance of 0.5-5 m for car digital keys, the AOA positioning error is ≤ 1.4°, so it can be used as the signal transceiver antenna of the AOA positioning system.

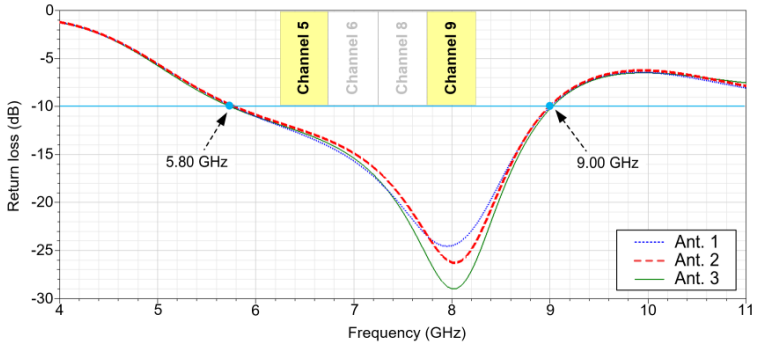

Figure 4. Simulated return loss of the proposed antenna.

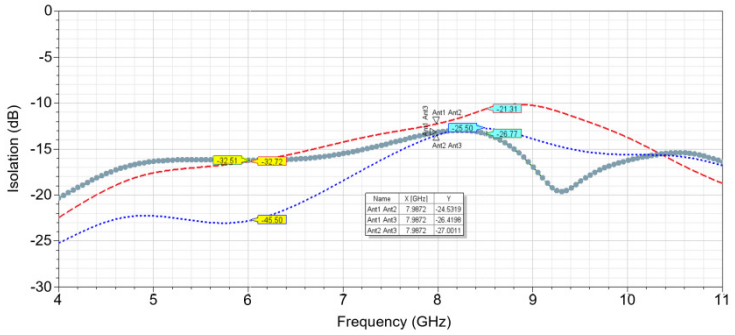

Figure 5. Isolation of the proposed antenna.

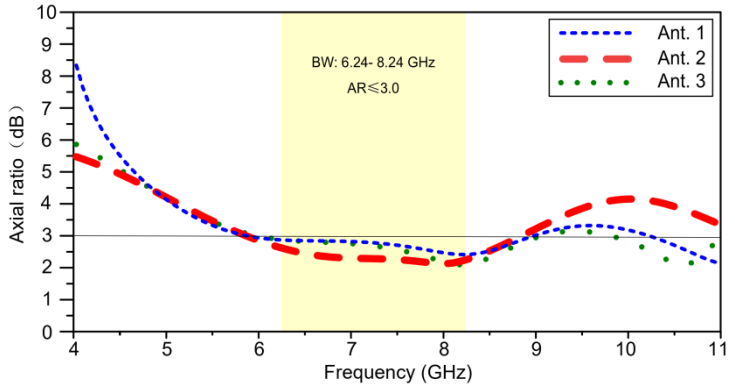

Figure 6. Axial ratio of the proposed antenna.

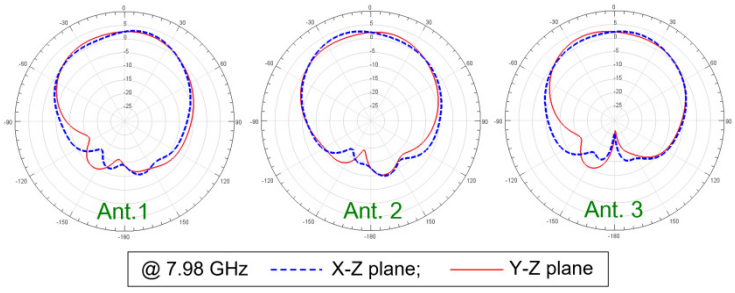

Figure 7. Radiation patterns of the proposed antenna.

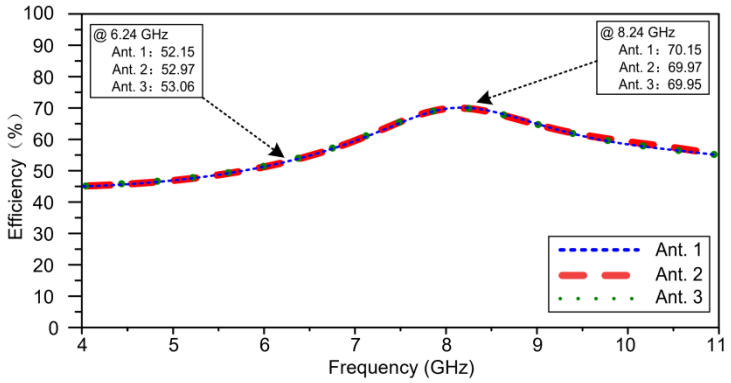

Figure 8. Efficiency of the proposed antenna.

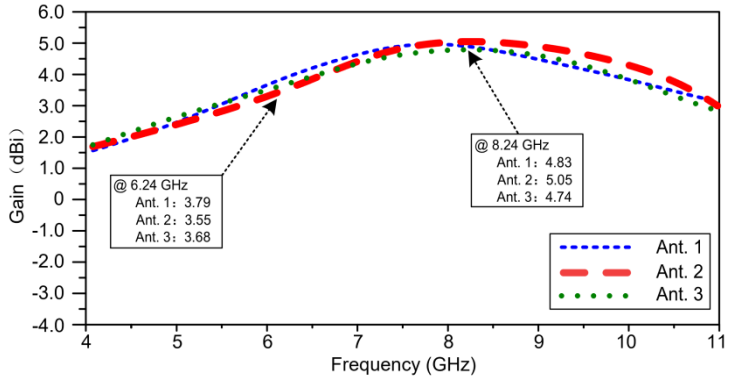

Figure 9. Gain of the proposed antenna.

4. Conclusion

This paper adopts a rectangular dual-feed microstrip patch structure to design an L-shaped array UWB circularly polarized antenna, and uses a simplified 90° feeding network to ensure circular polarization performance. The overall size is 42 mm × 40 mm × 2 mm, which fits the installation space of the digital key shell. The angle range covers 0° to 360° azimuth and -35° to 30° elevation, meeting the needs of contactless unlocking from different directions. The gain is stable at 3.55–5.05dBi, and the port isolation is controlled below -21.31dB. At the same time, it improves the ability to resist on-board electromagnetic interference and reduces the impact of metal shielding of the shell on antenna performance. The phase deviation is controlled within 4°, ensuring phase and amplitude consistency. Combined with the high polarization purity of the dual-feed array elements, the AOA positioning error is ≤ 1.4°, achieving high-precision positioning to meet the needs of automotive digital keys.

Disclosure statement

The authors declare no conflict of interest.

References

[1] Liu T, Wang J, 2024, A Digital Key Solution for Vehicles by UWB and BLE. Electronic Design Engineering, 32(18): 12–17.

[2] Ye X, Song J, Dou J et al., Design of Ultra-wideband Circularly Polarized Antenna for ETC Systems. Journal of Microwaves, 40(S1): 44–47.

[3] Wan M, Chen S, Wang T, et al., 2022, A Broadband Circularly Polarized Antenna Array for UWB, 2022 National Conference on Microwaves and Millimeter Waves, 844–846.

[4] Tan Z, et al., 2018, UWB-AOA Estimation Method Based on a Spare Antenna Array with Virtual Element, 2018 IEEE International Conference on Computational Electromagnetics (ICCEM), 1–3.

[5] Zhang Z, Lin Y, Jin B, 2021, Underwater TDOA/AOA Joint Localization Algorithm Based on Hybrid Invasive Weed Optimization Algorithm. IET Communications, 15(19): 2376–2389.

[6] Märzinger D, Etzlinger B, Peterseil P, et al., 2024, Compressive Sampling Enabled UWB AOA Estimation for IoT Applications, IEEE Globecom Workshops (GC Wkshps), Cape Town, 1–5.

[7] Zhang H, Liu X, Gulliver T, et al., 2013, AOA Estimation for UWB Positioning Using a Monostation Antenna Array. Journal of Electronics & Information Technology, 35(8): 2024–2028.

[8] Yang X, Fu J, Dong Y, et al., 2011, Study of Microwave Power Dividers with Phase Shifter. Proceedings of the 2011 National Conference on Microwaves and Millimeter Waves, 2011(1): 32–34.

[9] Gordebeke G, Lemey, S, Rogier, H, 2025, Metal-stamped and IR-UWB-optimized Air-filled Cavity-backed Antenna Array for Cost-effective Single-anchor 3d Localization. Access, IEEE, 2025(13): 125016–125028.

[10] Wang Y, 2021, Circularly Polarized Antenna Technology, De Gruyter, Berlin.

[11] Bancroft R, 2019, Microstrip and Printed Antenna Design (3rd Edition), IET Digital Library.

[12] Kang Y, Liu C, Wu H, Simulation Calculation and Optimization of Ternary Microstrip Antenna Array with Center Frequency of 915 MHz. Communications Technology, 51(7): 1722–1729.

[13] Wang Z, Liu Y, 2015, Simulation and Design of UHF Dual-Feed Microstrip Ceramic Antenna. Electronic Technique, 44(1): 45–46.

[14] Zeng B, Zhu H, 2024, Designing a Dual-feed Circular Polarization Antenna. Journal of Electronic Research and Application, 8(3): 255–261.

[15] Wang X, Li Y, Jiang H, 2008, Design and Simulation of Dual-Feed Circular Polarization Patch Antenna. Electronic Science and Technology, 2008(8): 12–13 + 16.

[16] Li J, Yu B, Yang M, et al., 2025, Deep Bayesian Neural Networks for UWB Phase Error Correction in Positioning Systems. Scientific Reports, 15(1): 1–12.